

Preparation of Thermosensitive, Calix[4]arene Incorporated P(NIPAM-*co*-HBCalix) Hydrogel as a Reusable Adsorbent of Nickel(II) Ions

Fanyong Yan, Meng Wang, Donglei Cao, Shanshan Guo, Li Chen

State Key Laboratory of Hollow Fiber Membrane Materials and Processes, Key Lab of Fiber Modification & Functional Fiber of Tianjin, Tianjin Polytechnic University, Tianjin, 300387 People's Republic of China

Correspondence to: L. Chen (E-mail: yfany@163.com)

Received 15 November 2012; accepted 29 January 2013; published online 15 March 2013

DOI: 10.1002/pola.26625

ABSTRACT: A calix-conjugated thermo-responsive hydrogel containing 15% tetra(5-hexenyloxy)-*p*-tert-butylcalix[4]arene (HBCalix), P(NIPAM-*co*-HBCalix), was used to remove nickel(II) ions from water. Both thermo-sensitive properties and the Ni²⁺-adsorption capabilities of the prepared P(NIPAM-*co*-HBCalix) hydrogels are investigated. Introduction of the monomer HBCalix considerably enhanced the adsorption of Ni²⁺ onto the hydrogel by chelation between hexenyloxy groups and metal ion. When HBCalix units capture Ni²⁺ and forms HBCalix/Ni²⁺ host-guest complexes, the lower critical solution temperature of the hydrogel shifts to a higher temperature due to both the repulsion between charged HBCalix/Ni²⁺ groups and the osmotic pressure within the hydrogel. Adsorption studies

were carried out by varying contact time, counter ion and initial concentration of Ni²⁺. The evaluation of adsorption properties showed that the hydrogel exhibited better correlation with Langmuir isotherm model. P(NIPAM-*co*-HBCalix) could be used repeatedly with little loss in adsorption capacity by simply changing the environmental temperature. This kind of ion-recognition hydrogel is promising as a novel adsorption material for adsorption and separation of Ni²⁺ ions. © 2013 Wiley Periodicals, Inc. *J. Polym. Sci., Part A: Polym. Chem.* **2013**, *51*, 2401–2408

KEYWORDS: adsorption; Calix[4]arene; hydrogel; nickel(II) ions removal; N-isopropylacrylamide; supramolecular structures

INTRODUCTION The role of heavy-metal ions in environmental issues has become increasingly prominent because of their unique detrimental and non-biodegradable characteristics for the living organisms.¹ Among the toxic ions, the nickel, which is widely used in modern industry and catalytic processes, has been shown to exert many negative effects on human health and environment if it had been discharged without suitable treatment.^{2,3} Various techniques (e.g., ion exchange, adsorption, chemical precipitate, and membrane processes) were used to remove the nickel(II) ion from wastewater streams. Adsorption has been shown to be an economically feasible method because of its high efficiency, easy handling and availability of adsorbents.^{4,5} Several different types of materials have been investigated as adsorbents, among them amorphous silica, activated carbon, clays, zeolites, and polymers.^{6–8} However, these adsorptive materials are either ineffective or nonselective, when metal ions are present in the wastewater at low concentrations. So, the synthesis of adsorbents for the removal of Ni²⁺ from wastewater is a continuing research objective of environmental pollution-control processes.

Smart synthetic hydrogels are attracting growing research interests due to their three-dimensional (3D) networks and

swell well in water or organic solvents.⁹ Poly(N-isopropylacrylamide) (PNIPAM) and its derivative copolymers are widely studied thermo-sensitive hydrogels as solid-phase extraction adsorbents. These hydrogels performed a temperature-swing adsorption (TSA) toward metal ions,^{10,11} such as PNIPAM hydrogels showed an extractive affinity for Au³⁺¹² and Cu²⁺-surfactant complexes.¹³ The modified PNIPAM hydrogels can bind heavy metal ions through different metal-complexing ligands, which interact selectively and strongly with heavy-metal ions.^{14–17} Moreover easy handling and reusability make hydrogels promising materials for water purification. Thus, there remains a need to discover more selective ionophores and distribute them in the PNIPAM chain.

Calixarenes, the third generation of synthetic host compounds, have a remarkable recognition ability toward specific metal ions through coordination bonds, hydrogen bonds, and ionic bonds.^{18,19} Calixarenes with appended or pendant groups can be thought as useful latent hosts for toxicant recognition and separation.^{20,21} When the ion diameter matches the cavity size of modified calix[4]arenes cavity, the ion could be captured by the calixarenes as receptors and

“host-guest” complexes are stably formed. Many advanced polymer materials for metal ion detection and selective separation have been designed by anchoring calixarenes derivatives to a polymeric support or bonding in the polymer backbone.²² Ulewicz et al.²³ studied the polymer inclusion membranes using calix[4]crown-6 derivatives as ion carriers and investigated their selectivity of Zn^{2+} , Cd^{2+} , and Pd^{2+} . Akkus et al. synthesized the polymeric calix[4]arene having phthalimide groups at the lower rim.²⁴ The order of extractability of metal cations by this derivative is selective in the sequence: $\text{Hg}^{2+} > \text{Cd}^{2+} > \text{K}^{+} > \text{Co}^{2+} > \text{Cu}^{2+}$. The central challenge in employing calixarenes in adsorptive materials is how best to secure them onto a polymeric support. Covalent linkages are ideal, but may require synthesis of the starting reagent given a suitable precursor is commercially available.

In this study, we prepared a novel thermo-sensitive poly (N-isopropyl acrylamide-co-tetra(5-hexenyloxy)-p-tert-butylcalix[4]arene) (P(NIPAM-co-HBCalix)) with good ion-recognition property by using PNIPAM hydrogel as an actuator and tetra(5-hexenyloxy)-p-tert-butylcalix[4]arene (HBCalix) as the ion-signal receptor. When the ambient temperature is lower than the lower critical solution temperature (LCST), PNIPAM chain stretching, HBCalix and Ni^{2+} with larger binding coefficient, more Ni^{2+} ions form complexes with the HBCalix, which are adsorbed on the hydrogel. Therefore, here we report the application of P(NIPAM-co-HBCalix) hydrogel as a novel adsorbent to remove Ni^{2+} from aqueous solutions.

EXPERIMENTAL

Materials

N-Isopropylacrylamide (NIPAM, Tokyo Kasei Kogyo, Japan) was purified by recrystallization with a cyclohexane-toluene (v/v, 50/50) mixture solution. Initiator 2,2'-azobisobutyronitrile (AIBN, Shanghai Siweihe Chemical, China) was recrystallized from ethanol solution. Cross-linker N,N'-methylenebisacrylamide (BIS, Tianjin Chemical Reagent, China). All other reagents for synthesis were purchased from commercial suppliers and used without further purification. The deionized water was prepared by a Millipore Nano Pure purification system (resistivity higher than $18.2 \text{ M}\Omega \text{ cm}^{-1}$).

Synthesis of HBCalix

P-tert-butylcalix[4]arene and HBCalix were synthesized according to the literature procedures.^{25,26} The mixture of p-tert-butylcalix[4]arene (0.05 mol), 6-bromo-1-hexene (0.50 mol), and anhydrous NaH (0.25 mol) in dimethyl sulfoxide (200 mL) were reacted at room temperature for 72 h under nitrogen atmosphere. The mixture was treated with HCl (10%, v/v) and extracted with CHCl_3 . The organic layer was separated, dried with MgSO_4 , and concentrated. The crude product was purified by column chromatography (silica gel, dichloromethane: petroleum ether = 2:1–10:3, v/v) to afford HBCalix as a white powder in 32% yield.

^1H NMR (300 MHz, CDCl_3): δ = 7.64 (s, 2H), 7.03 (s, 4H), 6.83 (s, 2H), 6.82 (s, 2H), 6.23(m, 1H), 5.75 (d, J = 15 Hz, 1H), 5.36 (d, J = 15 Hz, 1H), 4.52 (d, J = 2.0 Hz, 2H), 4.28

(d, J = 12.5 Hz, 4H), 3.95 (t, J = 7.5 Hz, 3H), 3.29 (d, J = 12.5 Hz, 4H), 2.02 (m, 2H), 1.27 (s, 18H), 1.24 (t, J = 7.5 Hz, 3H), 0.98 (s, 18H); ^{13}C NMR: δ = 150.8, 150.0, 149.9, 146.9, 146.8, 141.4, 133.2, 132.9, 127.9, 127.8, 125.6, 125.5, 125.1, 117.5, 33.9, 31.9, 31.8, 31.2, 23.5, 11.0; FT-IR (KBr, cm^{-1}): ν = 3413, 2961, 2904, 1643, 1486, 1361, 1120.

Preparation and Characterization of P(NIPAM-co-HBCalix) Hydrogels

Cross-linked P(NIPAM-co-HBCalix) hydrogels were prepared by thermally initiated free-radical copolymerization.²⁷ NIPAM (3.3942 g), HBCalix (0.5512 g) and crosslinker fully dissolved in 20 mL mixed solvent CH_2Cl_2 - CH_3CN (v/v, 1/1) using AIBN as initiator. The polymerization was carried out at 60 °C for 12 h under nitrogen atmosphere. The pure PNIPAM hydrogel was prepared under the same condition, but without any addition of HBCalix. After the gelation was completed, the P(NIPAM-co-HBCalix) hydrogels obtained was cut into circular pieces (1.0 cm in diameter) with a perforator. Hydrogel disks were soaked in ethanol and deionized water overnight to remove any remaining unreacted monomers or initiator. This rinsing step was repeated three times and then stored in Millipore water at 12 °C.²⁸ Before the measurements, the originally swollen hydrogels samples were dried in an oven to a constant weight at 40 °C for 48 h and then freeze-dried by FD-1TC freeze dryer (−45 °C and 0.1 mbar) for at least 48 h. The samples were kept in a closed container for characterization and for use in the adsorption experiment.

The FT-IR analyses of powdered xerogel samples were characterized by Nicolet 560 spectrophotometer. The proper amount ratio (Sample:KBr = 1:50) was mixed and grounded and then compressed into a pellet under a pressure of 11 tones, for about a minute, using a Graseby Specac Model: 15.011. Spectra were obtained in the 4000–400 cm^{-1} wave number range, at 25 °C and at 4 cm^{-1} spectral resolution. Proton Nuclear magnetic resonance spectroscopy (^1H NMR) experiments were performed on a Bruker DRX-300 NMR spectrometer with DMSO-d_6 as solvent and TMS as the internal standard. Carbon nuclear magnetic resonance (^{13}C NMR) spectra was recorded on the Bruker DSX-400 NMR spectrometer operated at a resonance frequency of 100.47 MHz. Scanning electron microscopy (SEM) images were collected on a JEOL JSM-6380 electron microscope.

Metal ions Adsorption and Thermo-Sensitive Behaviors of P(NIPAM-co-HBCalix) Hydrogels

The ion-recognition and thermo responsive behaviors of P(NIPAM-co-HBCalix) hydrogels are comprehensively investigated by evaluating their volume-phase transition (VPT) behaviors in metal ion (Ni^{2+} , Pb^{2+} , Cd^{2+} , and Cu^{2+}) solutions and deionized water. For this purpose, aqueous solutions (10 mL) containing different amounts of metal ions (in the range of 1–40 mg L^{-1}) were incubated with 0.05 g dried hydrogels at various designed ambient temperature values. After the desired adsorption period (up to 180 min), concentration of metal ion in the aqueous phases was

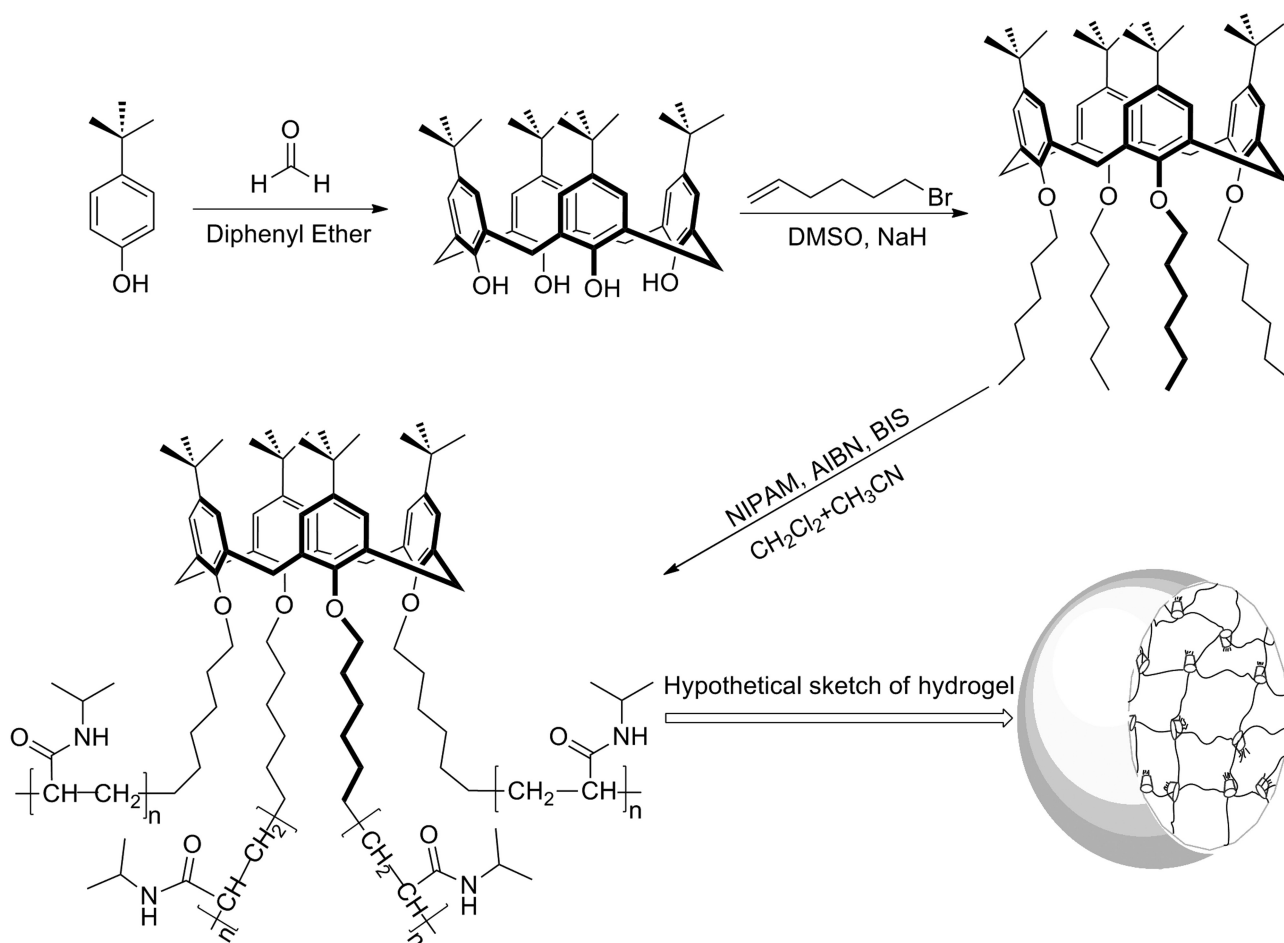


FIGURE 1 Schematic representation of the synthesis of HBCalix and its corresponding polymeric P(NIPAM-*co*-HBCalix) hydrogels.

measured using inductively coupled plasma (ICP, Atomscan Advantage). A water-bath shaker (model CH-4311) at a speed of 150 rpm was used throughout the equilibrium examination.

The equilibrium amounts of metal ions adsorbed onto the unit mass of P(NIPAM-*co*-HBCalix) hydrogels at the designed temperature T ($^{\circ}\text{C}$), Q (mg g^{-1}), was determined using the mass balance equation as follows:

$$Q = [(C_0 - C_e) \cdot V] / m \quad (1)$$

where V is the volume of the solution (L), and m is the weight of the dried P(NIPAM-*co*-HBCalix) gel (g), respectively; C_0 and C_e (mg L^{-1}) are the initial and equilibrium concentrations of the metal ions in the aqueous phase after adsorption at T ($^{\circ}\text{C}$). For comparison, similar adsorption experiments are also carried out with PNIPAM hydrogels. To obtain the reusability of P(NIPAM-*co*-HBCalix) hydrogels, adsorption-desorption cycle was repeated five times using the same adsorbent in a batch system. Desorption of Ni^{2+} from P(NIPAM-*co*-HBCalix) hydrogels was achieved by using 10 mL deionized water. The hydrogels were placed in the desorption medium and shaken in a water bath shaker at a

rate of 150 rpm for 180 min. The concentration of Ni^{2+} ions in the desorption medium were followed as described before. After each adsorption-desorption cycle, the P(NIPAM-*co*-HBCalix) hydrogels were washed three times in 50 mL of deionized water to eliminate metal ions that were not bound to the hydrogel matrix. Rinses took 6 h and were stopped when the rinse solution contained no Ni^{2+} ions detectable by ICP mass spectrometry.

RESULTS AND DISCUSSION

Characterization Studies

The synthesis route of P(NIPAM-*co*-HBCalix) hydrogels is shown in Figure 1. A 3D hydrogel network formed in 30 min. The HBCalix content in the hydrogel was generally 12.2% (W/W). Uncrosslinked HBCalix content was verified by means of soaking the hydrogel in methanol at ambient temperature for 1 or 4 days followed by HPLC analysis of the soak solutions. The hydrogel sample is transparent at lower temperature 12 $^{\circ}\text{C}$. By visual appearance the same hydrogel suddenly turns into white color from transparent near 32 $^{\circ}\text{C}$. It is known that the sequential distribution is mainly depended on the relative reactivity ratio of the

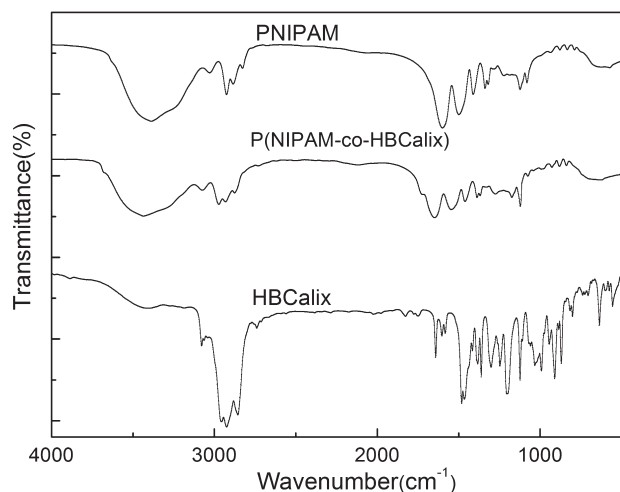


FIGURE 2 FT-IR spectra of HBCalix, PNIPAM and P(NIPAM-co-HBCalix) hydrogel.

monomers and the monomer feed ratio.²⁹ Hydrogels containing more amounts of HBCalix were directly synthesized. However, these hydrogels had a poor mechanical strength. The reason may be that too much HBCalix monomers isolated the hydrogel chains and prevented them from forming hydrogen bonds, which limited the primary source of the physical cross-links in the hydrogels.³⁰

The FT-IR spectra of P(NIPAM-co-HBCalix) and PNIPAM hydrogels as well as HBCalix monomer is shown in Figure 2. Evidently, the FT-IR spectra of all the hydrogels was similar, although the spectrum of each hydrogel showed slight changes with different HBCalix contents. Every spectrum showed a broad band in the range of 3600–3200 cm^{-1} , which belongs to N–H stretching vibration of the NIPAM. A strong band around 2920 cm^{-1} can be assigned as stretching vibrations of $-\text{CH}_2-$ from NIPAM and HBCalix. The typical amide I band (1650 cm^{-1}), consisting of C=O stretch of PNIPAM and amide II bands (1540 cm^{-1}), including N–H vibration are evident in every spectrum.³¹ Two bands of C–H vibration at 1386 and 1367 cm^{-1} belong to the divided bands of the symmetric $-\text{CH}(\text{CH}_3)_2$ group. The existence of HBCalix was evident by the presence of a strong 1460 cm^{-1} band for C=C skeletal stretching vibration of phenyl ring³²; consisting of C–O asymmetric stretching vibration in R–O–R', although this band was weak due to the low HBCalix content in hydrogels. The peak intensity at 1120 cm^{-1} increased gradually, which confirmed that the HBCalix content increased. All above are important evidence to prove that P(NIPAM-co-HBCalix) hydrogels were polymerized successfully.

Solid state ^{13}C NMR spectroscopy provides information regarding the structure of P(NIPAM-co-HBCalix). Figure 3 displays ^{13}C NMR spectra of P(NIPAM-co-HBCalix) and PNIPA. The feature signal at 31 ppm corresponding to P(NIPAM-co-HBCalix) is the carbon of tert-butyl. Solid-state ^{13}C -NMR of PNIPAM shows three broad peaks at 20–26 ppm ($-\text{CH}_3$, NIPAM; $-\text{CH}-$ backbone), 30–50 ppm ($-\text{CH}-$

and $-\text{CH}_2-$ backbone and $-\text{CH}-\text{N}-$ NIPAM) and 170–180 ppm (CO, NIPAM). The ^{13}C NMR spectra provided further evidence for the formation of P(NIPAM-co-HBCalix) copolymer between HBCalix and NIPAM.

The cross-section structures of freeze-dried hydrogels by SEM are shown as Figure 4. The data clearly illustrate the dependence of interior morphology on the composition ratio of HBCalix. From the size of the bar, these hydrogel networks have a different porous structure. PNIPAM hydrogel [Fig. 4(a)] has the smallest one in the range of 25–50 μm , while P(NIPAM-co-HBCalix) hydrogel [Fig. 4(b)] has been large continuous interconnected pore size in the range of 70–160 μm . Because of numerous interconnected pores in the hydrogel network, water molecules can easily diffuse. P(NIPAM-co-HBCalix) hydrogels could enhance the rate of the swelling processes. The thermosensitive P(NIPAM-co-HBCalix) hydrogels have potential applications in the extraction of metal ions since the network may be able to provide enough space for the loading and releasing of metal ions. The formation of macroporous structures of P(NIPAM-co-HBCalix) can be explained by the following: the network structure of P(NIPAM-co-HBCalix) hydrogels are different, mainly due to the HBCalix contains four aromatic rings linked by methylene bridges, a highly expanded network can be generated by electrostatic repulsion among hydrophobic cavities during the polymerization process. Therefore, the sizes of pores over range from 50 to 160 μm that increase the interaction between hydrogel and the metal ions and decrease the diffusion limitation in metal ion's adsorption. The similar phenomenon is also reported.¹⁰

Single-Component Heavy Metal Ions Adsorption Rate of P(NIPAM-co-HBCalix) Hydrogels

The effect of contact time on adsorption values of metal ions on P(NIPAM-co-HBCalix) hydrogel was studied, and the results are presented in Figure 5. It is observed that P(NIPAM-co-

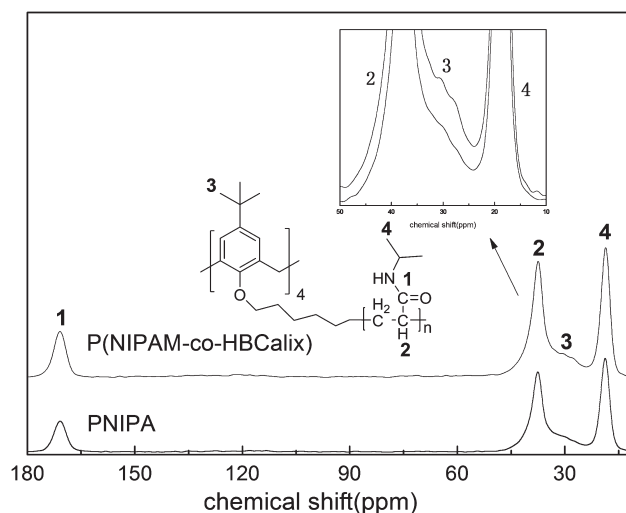


FIGURE 3 ^{13}C NMR spectra of PNIPAM and P(NIPAM-co-HBCalix) hydrogel.

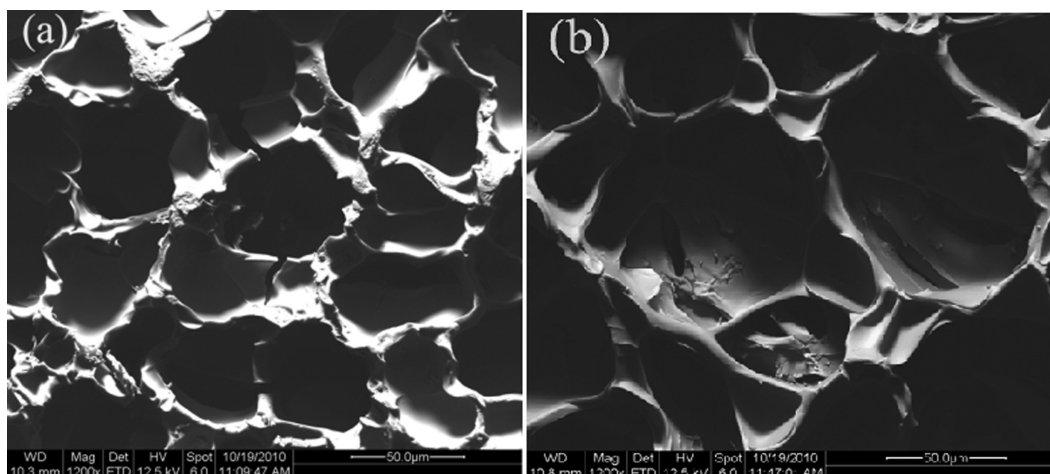


FIGURE 4 SEM images of PNIPAM hydrogel (a), P(NIPAM-*co*-HBCalix) hydrogel (b) freeze-dried at low temperature.

HBCalix) hydrogels show a significant extraction ability toward transition metal cations Ni^{2+} , Cu^{2+} , Pb^{2+} , Zn^{2+} . Where the adsorption occurred in two steps, the initial adsorption rates increases sharply during the first 1 h, followed by gradually establishing adsorption equilibrium (plateau values) within 150 min for all the tested metals. This fast adsorption equilibrium is most probably due to high complexation and geometric affinity between functional calix groups and heavy-metal ions. The equilibrium was reached within 150 min. As seen in the figure, high adsorption capacity for Ni^{2+} (3.481 mg g^{-1}) was achieved with P(NIPAM-*co*-HBCalix) hydrogels. Further increase in contact time did not show an increasing in adsorption. Thus, 150 min shaking time was considered to be the optimum contact time for adsorption of metal ions on P(NIPAM-*co*-HBCalix) hydrogels. In particular, there are no chelating functional groups on the plain PNIPAM hydrogels, the adsorption of mental ions on PNIPAM hydrogels was low at 10 or 50°C.³³ This adsorption may be due to diffusion of metal ions into the matrix and weak interactions between metal ions and amide moieties of PNIPAM hydrogels. Therefore, this result means that introducing hexenyloxy groups to the calixarene platform is essential for creating a high extractability for Ni^{2+} ions.

Ion-Recognition and Thermo-sensitive Behaviors of P(NIPAM-*co*-HBCalix) Hydrogels

In this work, all the hydrogels can be swollen without dissolving, suggesting the formation of crosslinked structures. It is seen that at a low temperature (e.g., $<30^\circ\text{C}$) the final hydrogels obtained were macroscopically homogeneous surface and translucent in appearance. When heated up to the higher temperatures (e.g., $>40^\circ\text{C}$), the hydrogels became shrank and cloudy, implying the occurrence of the VPT phenomenon. Re-cooled to the low temperatures, the hydrogels can be re-swollen and became translucent again. This observation indicates that all P(NIPAM-*co*-HBCalix) hydrogels possess temperature-sensitive properties.

The Ni^{2+} -recognition and thermo responsive characteristics of hydrogels with different HBCalix contents are studied by

detecting the volume change in deionized water and in $20 \text{ mg L}^{-1} \text{ Ni}^{2+}$ aqueous solutions. Where V_T/V_0 is the ratio of volume of the hydrogel disc at temperature T to that at 21°C . The temperature, at which the value of V_T/V_0 decreases to half of the total change value, is taken as the LCST of the cross-linked hydrogel. As shown in Figure 6(a,b), the volume-change trend of PNIPAM hydrogels is almost the same as that in Ni^{2+} solution, and the LCST of PNIPAM hydrogel in Ni^{2+} solution does not have any significant change compared with that in deionized water. The result indicates that the metal ions scarcely affect the phase transition behaviors of PNIPAM-based hydrogels without presence of HBCalix receptors in the polymeric networks.

As expected, the temperature-dependent volume-change trend of P(NIPAM-*co*-HBCalix) hydrogels in Ni^{2+} solution is significantly different from that in deionized water. The LCST of P(NIPAM-*co*-HBCalix) hydrogel shifts to a higher temperature in Ni^{2+} solution: the P(NIPAM-*co*-HBCalix) hydrogel

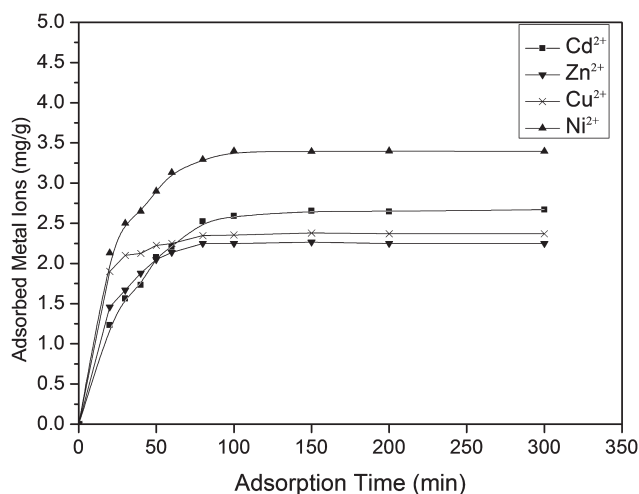


FIGURE 5 Adsorption rates of metal ions on P(NIPAM-*co*-HBCalix) hydrogel; initial concentration of metal ions 20 mg/L, temperature: 21°C and pH: 6.0.

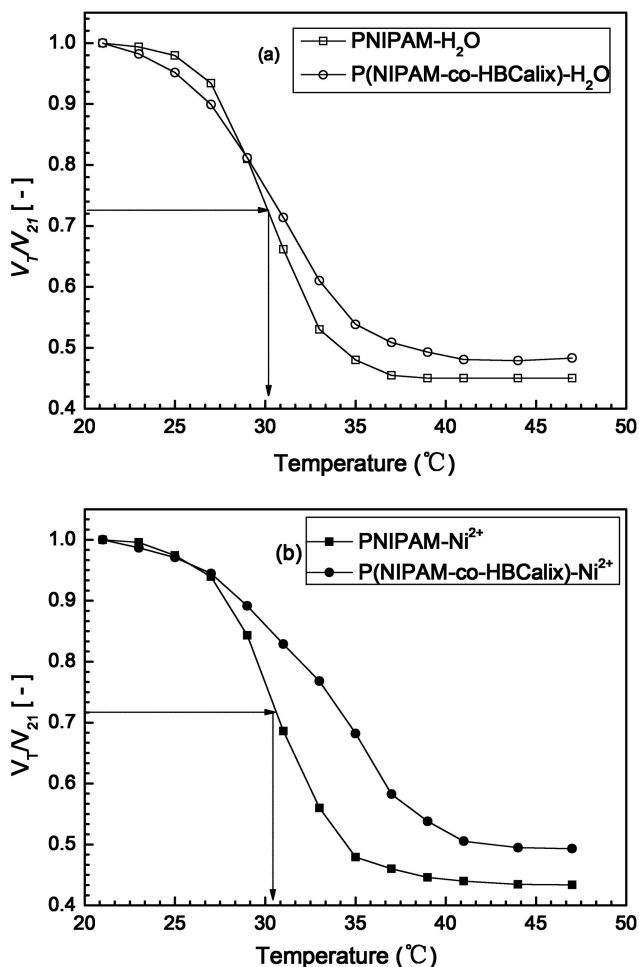


FIGURE 6 Temperature dependence of volume change ratios of P(NIPAM-*co*-HBCalix) and PNIPAM hydrogels in deionized water and Ni²⁺ aqueous solution (20 mg/L) (a-b).

shifts to 33.5 °C. Such an LCST shift indicates the HBCalix receptors in the copolymer hydrogel can recognize and effectively capture Ni²⁺ into their cavities, and then the formation of supramolecular “host-guest” HBCalix/metal ion complexes. The repulsion between charged HBCalix/Ni²⁺ complexes

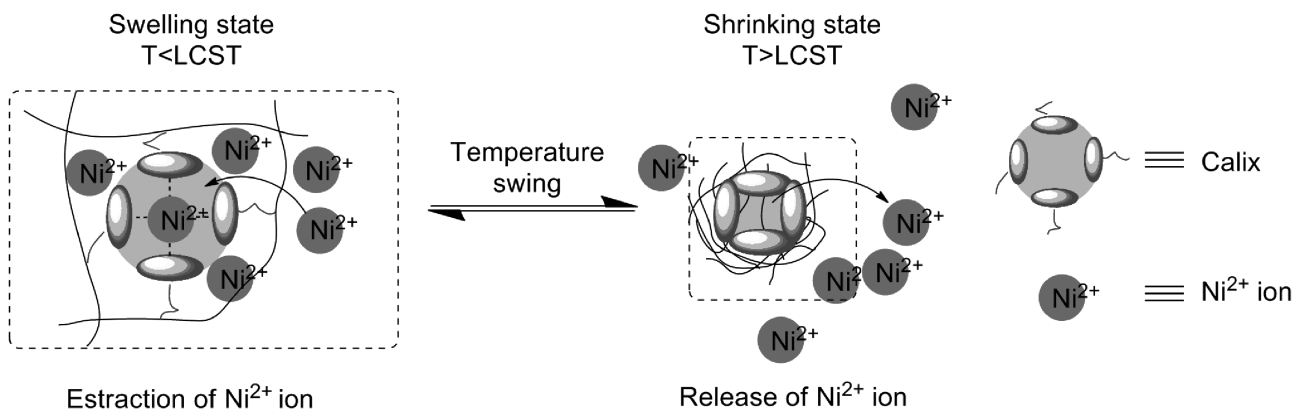


FIGURE 7 Concept of the thermal-responsive adsorption/desorption behavior of P(NIPAM-*co*-HBCalix) hydrogel towards Ni²⁺ ions.

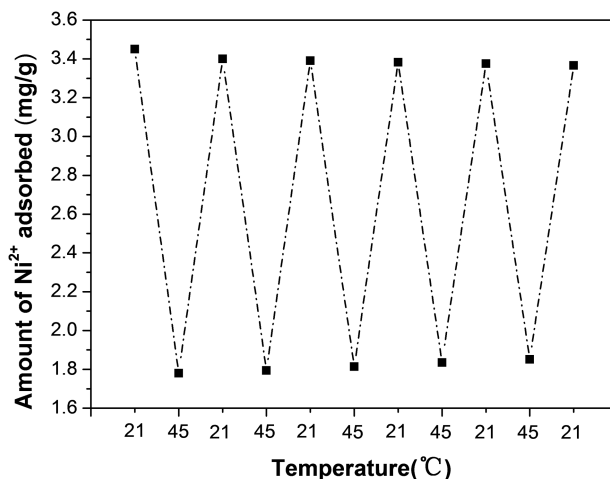


FIGURE 8 Observed amounts of Ni²⁺ ions adsorbed on the P(NIPAM-*co*-HBCalix) hydrogels at 21 °C and 45 °C during the temperature swing.

counteract the shrinkage of P(NIPAM-*co*-HBCalix) hydrogels like ionic polymer networks during the increase of temperature. Additionally, the osmotic pressure within the hydrogel due to a Donnan potential also makes the hydrogel swell more when the temperature is high enough, thereby resulting in the shift of the LCST to a higher temperature.

It can be said that the change in the size of hydrogel-network or the hydrophilic/hydrophobic transition has an important effect on adsorption performance. At temperature lower than the LCST, P(NIPAM-*co*-HBCalix) hydrogels swell and there is small steric hindrance near the HBCalix cavities but can provide a room to accept Ni²⁺ ions, which lead to Ni²⁺ ions easily be included into the HBCalix cavities with the 5-hexenyloxy groups. The swollen network structure can provide enough space so that the complex of HBCalix cavity and Ni²⁺ ion is comparatively high at temperature lower than the LCST. This decrease in adsorption of P(NIPAM-*co*-HBCalix) hydrogels can be attributed to the existence of multifunctional groups in HBCalix such as four aromatic rings

TABLE 1 Langmuir and Freundlich Adsorption Isotherm Constants of P(NIPAM-co-HBCalix)

Type	Langmuir Isotherm			Freundlich Isotherm		
	q_m (mg g ⁻¹)	b (L g ⁻¹)	R^2	K_F	$1/n$	R^2
Ni	3.9908	2.8598	0.9936	2.8135	0.3825	0.9881

linked by methylene bridges and hexenyloxy groups, which are grafted onto the hydrogels. Therefore, more interactions with the ions take place. When at temperature higher than the LCST, the leveling off of adsorption amount after a certain graft yield is due to the densely packed structure of hexenyloxy groups which acts as a barrier after a certain value of grafting that impedes diffusion of ions into the HBCalix backbone. A schematic illustration of the thermo-responsive adsorption/desorption behavior of P(NIPAM-co-HBCalix) hydrogels toward Ni²⁺ ion is shown in Figure 7. This phenomenon verifies that P(NIPAM-co-HBCalix) hydrogels can be applied to temperature-controlled Ni²⁺ separation.

Desorption and Repeated Use

To examine the stability of adsorption performance of P(NIPAM-co-HBCalix) hydrogels by repeating temperature swing, the temperature was changed repeatedly between 21 and 45 °C, and the adsorbed amount was measured using the same the P(NIPAM-co-HBCalix) hydrogels. The result is shown in Figure 8. The amount adsorbed is high at 21 °C and low at 45 °C, that is, the P(NIPAM-co-HBCalix) adsorbs and desorbs reversibly. It can be considered that in metal chelating systems, chelation (i.e., binding of heavy-metal ion with HBCalix) is completely reversible. After each adsorption-desorption cycle, the hydrogels were washed several times with deionized water. The amount adsorbed at 21 °C seems to decrease somewhat due to the repetition of TSA. As the adsorption amount is mg g⁻¹ level, when the concentration of Ni²⁺ ions is detected by ICP, the volume of solution will be lost, even the loss is trace amounts, the amount adsorbed at 21 °C seems to decrease somewhat. The result showed the feasibility of the P(NIPAM-co-HBCalix) hydrogels for Ni²⁺ ion recovery.

Adsorption Isotherms

An equilibrium isotherm is used to characterize the interaction of Ni²⁺ with P(NIPAM-co-HBCalix) hydrogels. This represents the relationship between the amount of adsorbate removed from solution and unit of mass of a sorbent, at the constant temperatures, at equilibrium. In this work, the Ni²⁺ ions initial concentration was varied from 1 to 20 mg L⁻¹ with 24 h of contact time to obtain the experimental adsorption data. Results were fitted by two parameter Langmuir (eq (2)) and Freundlich (eq (3)) models,

$$q_e = q_m b C_e / (1 + b C_e) \quad (2)$$

$$q_e = K_F C_e^{1/n} \quad (3)$$

where q_e is the adsorbed amount of the Ni²⁺ ions (mg g⁻¹), q_m is the maximum adsorption capacity (mg g⁻¹), C_e

is the equilibrium Ni²⁺ concentration in solution (mg L⁻¹), b is the constant eluted to the affinity binding sites (L mg⁻¹), K_F is the Freundlich constant, and n is the Freundlich exponent.

Table 1 shows the values of the parameters of the two isotherms and the related correlation coefficients. Langmuir model fits better to the produced data than Freundlich model according to R^2 values. Langmuir isotherm assumes monolayer adsorption onto a surface containing finite number sites of uniform strategies of adsorption with no transmigration of adsorbate in the plane of surface.³⁴ As also illustrated in Table 1, the value of $1/n$ is 0.3825, which indicates favorable adsorption.³⁵ Therefore, the Langmuir model can be applicable in Ni²⁺ ions removal by P(NIPAM-co-HBCalix) hydrogels.

CONCLUSIONS

Smart thermo-sensitive P(NIPAM-co-HBCalix) hydrogels capable of recognizing metal ions have been successfully developed in this study. The prepared P(NIPAM-co-HBCalix) hydrogels exhibit good Ni²⁺ adsorption characteristics by the HBCalix units. The LCST of the P(NIPAM-co-HBCalix) hydrogel shifts to 33.5 °C due to the formation of HBCalix/Ni²⁺ host-guest chelating sites. The swollen hydrogel can provide enough space so that the adsorption amount is comparatively high at temperature lower than the LCST. The adsorption of Ni²⁺ onto the hydrogels reached equilibrium within about 150 min. When at temperature higher than the LCST, the hydrogel chains shrink more drastically, and it is so crowded around the HBCalix cavities, the complex becomes unstable leading to Ni²⁺ desorption. The experimental adsorption data could be better fitted by Langmuir isotherm model rather than Freundlich model. After five adsorption-desorption cycles, the adsorption capacity could be maintained above 90% with no significant loss in adsorption properties.

ACKNOWLEDGMENTS

The authors thank the financial supports from the National Natural Science Foundation of China (50973084), Science and Technical Development Foundation of Colleges and Universities, Tianjin, China (20071214).

REFERENCES AND NOTES

- H. Pahlavanzadeh, A. R. Keshtkar, J. Safdari, Z. Abadi, *J. Hazard. Mater.* **2010**, *17*, 5304–310.
- K. Mitsudo, T. Imura, T. Yamaguchi, H. Tanaka, *Tetrahedron Lett.* **2008**, *49*, 7287–7289.
- C. Zhong, T. Sasaki, M. Tada, *J. Catal.* **2006**, *242*, 357–364.
- E. Katsou, S. Malamis, K. J. Haralambous, M. Loizidou, *J. Membr. Sci.* **2010**, *360*, 234–249.
- P. Zhao, J. Jiang, F. W. Zhang, W. F. Zhao, J. T. Liu, R. Li, *Carbohydr. Polym.* **2010**, *81*, 751–757.

- 6 Y. Xiong, H. T. Wang, Z. N. Lou, W. J. Shan, Z. Q. Xing, G. C. Deng, D. B. Wu, D. W. Fang, B. K. Biswas, *J. Hazard. Mater.* **2011**, *186*, 1855–1861.
- 7 S. R. Popuri, Y. Vijaya, V. M. Boddu, K. Abburi, *Bioresour. Technol.* **2009**, *100*, 194–199.
- 8 R. Singhon, J. Husson, M. Knorr, B. Lakard, M. Euvrard, *Colloids Surf. B: Biointerfaces* **2012**, *93*, 1–7.
- 9 X. J. Ju, L. R. Liu, R. Xie, H. C. Niu, L. Y. Chu, *Polymer* **2009**, *50*, 922–929.
- 10 A. Grimm, C. Nowak, J. Hoffmann, W. Scharl, *Macromolecules* **2009**, *42*, 6231–6238.
- 11 H. Tokuyama, A. Kanehara, *Langmuir* **2007**, *23*, 11246–11251.
- 12 H. Tokuyama, A. Kanehara, *React. Funct. Polym.* **2007**, *67*, 136–143.
- 13 A. G. Kilic, S. Malci, O. Celikbicak, N. Sahiner, B. Salih, *Anal. Chim. Acta.* **2005**, *547*, 18–25.
- 14 T. Ito, T. Yamaguchi, *Langmuir* **2006**, *22*, 3945–3949.
- 15 Y. Y. Liu, X. D. Fan, *Polymer* **2002**, *43*, 4997–5003.
- 16 A. Hrdina, E. Lai, C. S. Li, B. Sadi, H. Gary, *React. Funct. Polym.* **2012**, *72*, 295–302.
- 17 X. J. Ju, S. B. Zhang, M. Y. Zhou, R. Xie, L. H. Yang, L. Y. Chu, *J. Hazard. Mater.* **2009**, *167*, 114–118.
- 18 S. Memon, M. Tabakci, D. M. Roundhill, M. Yilmaz, *React. Funct. Polym.* **2006**, *66*, 1342–1349.
- 19 Y. Lu, C. C. Xiao, Z. F. Yu, X. S. Zeng, Y. Ren, C. X. Li, *J. Mater. Chem.* **2009**, *19*, 8796–8802.
- 20 F. Corbellini, R. Fiammengo, P. Timmerman, M. Crego-Calama, K. Versluis, A. J. R. Heck, I. Luyten, D. N. Reinhoudt, *J. Am. Chem. Soc.* **2002**, *124*, 6569–6575.
- 21 F. Corbellini, L. D. Costanzo, M. Crego-Calama, S. Geremia, D. N. Reinhoudt, *J. Am. Chem. Soc.* **2003**, *125*, 9946–9947.
- 22 A. J. M. Valente, A. Jiménez, A. C. Simões, H. D. Burrows, A. Y. Polishchuk, V. M. M. Lobo, *J. Eur. Polym.* **2007**, *43*, 2433–2442.
- 23 M. Ulewicz, U. Lesinska, M. Bochenska, M. Walkowiak, *Sep. Purif. Technol.* **2007**, *54*, 299–305.
- 24 G. U. Akkus, C. Cebeci, *J. Inclusion Phenom. Macrocycl. Chem.* **2008**, *62*, 303–309.
- 25 C. D. Gutsche, B. Dhawan, N. K. Hyun, *J. Am. Chem. Soc.* **1981**, *103*, 3782–3792.
- 26 G. McMahon, R. Wall, K. Nolan, D. Diamond, *Talanta* **2002**, *57*, 1119–1132.
- 27 S. Morisada, K. Namazuda, H. Kanda, Y. Hirokawa, Y. Nakano, *Adv. Powder Technol.* **2010**, *21*, 28–33.
- 28 Y. J. Huang, M. Z. Liu, L. Wang, C. M. Gao, S. S. Xi, *React. Funct. Polym.* **2011**, *71*, 666–673.
- 29 R. O. R. Costa, R. F. S. Freitas, *Polymer* **2002**, *43*, 5879–5885.
- 30 H. L. Liu, M. Z. Liu, L. W. Ma, J. Chen, *J. Eur. Polym.* **2009**, *45*, 2060–2067.
- 31 X. Z. Zhang, J. T. Zhang, R. X. Zhuo, C. C. Chu, *Polymer* **2002**, *43*, 4823–4827.
- 32 P. Mi, X. J. Ju, R. Xie, H. G. Wu, J. Ma, L. Y. Chu, *Polymer* **2010**, *51*, 1648–1653.
- 33 S. Hemvasdukij, W. Ngeontae, A. Imyim, *J. Appl. Polym. Sci.* **2011**, *120*, 3098–3108.
- 34 W. J. Weber, *Physicochemical Processes for Water Quality Control*; Wiley Intersci: New York, **1972**.
- 35 A. W. Adamson, A. P. Gast, *The Solid-Liquid Interface-Contact Angle, Physical Chemistry Surfaces*; Wiley and Sons, New York, **1990**: 379–420.